MAGNETOHYDRODYNAMICS Vol. 42 (2006), No. 2–3, pp. 199–206

VORTICITY GENERATION IN LOCALIZED MAGNETIC FIELDS

S. Cuevas[1], *S. Smolentsev*[2], *M. Abdou*[2]

[1] *Center for Energy Research, National University of Mexico*
A.P. 34, Temixco, Mor. 62580, Mexico
[2] *Mechanical and Aerospace Engineering Department, University of California*
Los Angeles, 44-114 Eng. IV, Los Angeles, CA 90095-1795 USA

The generation of vorticity in localized magnetic fields is explored under the low magnetic Reynolds number approximation. Analytic solutions for a creeping flow past a magnetic point dipole are obtained through a perturbation method. Also, numerical calculations for the flow past a finite size magnetic dipole are presented. It is shown that vortical structures may become unstable when inertial effects are not negligible.

Introduction. Non-uniformities are commonly used to generate vorticity in magnetohydrodynamic (MHD) flows. For instance, the use of solid obstacles in the flow under uniform magnetic fields has been widely explored both theoretically and experimentally to understand vortex formation and evolution [1, 2]. Vorticity can also be created under uniform fields through the expansion or contraction of duct geometry. Another interesting possibility of vortex generation in the channel flow under uniform fields is due to inhomogeneities in the electrical conductivity of the walls, as has been demonstarted by Alpher *et al.* [3] and Bühler [4].

It is also well known that vorticity can be generated due to fringing magnetic fields. In fact, most of the investigations of flows in fringing fields has been devoted to the analysis of duct flows with a field that varies in the streamwise direction as it approximately occurs at the entrance or exit of the poles of a magnet. In this case, current loops are elongated in the flow direction giving rise to streamwise current density components that produce Lorentz forces pointing towards the side walls. These forces are responsible for the creation of M-shape velocity profiles with high side-layer velocitites [5]. The strong shear layers created by the non-uniform field remain confined by the side walls, which determine their evolution inside or outside the magnetic field. Actually, in channel flows a non-uniform field acts as an electromagnetic brake, as those commonly used in metallurgical applications. It is then possible to visualize a non-uniform field as an obstacle for the flow and rise the question of how the flow evolution would develop in the absence of confining side walls. In experiments performed in a thin electrolytic layer with a localized moving magnetic field, Honji and Haraguchi [6, 7] demonstarted that generation of vorticity in inhomogeneous magnetic fields may lead to time-dependent flows with complex vortical structures. They used a shallow layer of salt water contained in a long tank with an electric current injected transversally to the tank axis. A permanent magnet located externally but close to the layer was moved at a constant velocity along the center line of the water tank. In the wake behind the region influenced by the field, different flow patterns including a wavy motion, symmetric vortex pairs and periodic vortex shedding were observed depending on the velocity of the magnets and the injected electric current [6, 7]. New experimental evidence was recently obtained by Afanasyev and Korabel [8]

using a similar device but considered flows produced by a single magnet as well as by two magnets with opposite orientations aligned with the direction of motion. In all these experiments flows exhibit features similar to those of ordinary flows around solid obstacles. However, a magnetohydrodynamic flow analysis is not accomplished.

In this paper, we explore the interaction of uniform flows with inhomogeneous magnetic fields. We are particularly interested in the evolution of shear layers created by localized gradients of magnetic field. With this aim, we analyze the flow of an incompressible electrically conducting viscous fluid past a localized zone of the applied magnetic field, denominated a *magnetic obstacle*. We introduce this term both to describe the obstruction found by the fluid as it moves through a zone of the localized non-uniform field and to emphasize the analogy with the flow past solid obstacles. In order to address the problem in a simplified way, we consider a 2D approach that retains the most important physical effects. A quasi-2D analysis including a localized Hartmann–Rayleigh friction has been addressed elsewhere [9]. It is shown that the flow past a magnetic obstacle can develop vortical structures and eventually instabilities that remind those observed in flows interacting with bluff bodies.

1. Formulation. We consider a uniform two-dimensional flow of an electrically conducting incompressible viscous fluid in a rectangular region, where a non-uniform distribution of magnetic field is present. The applied field, $\mathbf{B}^0$, is produced by a magnetized square surface uniformly polarized at the normal direction and slightly underneath from the plane of flow. Therefore, the dominant contribution of the applied field comes from the normal component. The area of this surface is only a small fraction of the total flow domain. Due to its fast decay, the field presents a high intensity only in a localized zone, which is assumed to be distant from the inlet/outlet region as well as from the lateral boundaries. At the entrance, a steady unidirectional flow with a uniform velocity profile, U, is imposed in the x-direction. Far from the region of intense field the flow is undisturbed. In the small zone, where the oncoming uniform flow encounters the non-uniform magnetic field, electric currents are induced, which, in turn, induce a field $\mathbf{b}$, so that the total magnetic field is given by $\mathbf{B} = \mathbf{B}^0 + \mathbf{b}$. We assume that the induced field is much smaller than the applied field, $\mathbf{b} << \mathbf{B}^0$, that means that the magnetic Reynolds number, $\mathrm{Rm} = \mu\sigma UL$, is much less than unity. Here, μ and σ are the magnetic permeability and the electric conductivity of the fluid, respectively, and L is a characteristic length to be defined below. Notice that the fluid passing through the magnetic obstacle faces mainly four different regions of the fringing magnetic field. In a similar way as in the flow at the entrance/exit of a magnet [5], closed current loops are formed in the plane of flow upstream and downstream of the applied field with clockwise and anti-clockwise current circulation, respectively. However, since side walls are absent current loops tend to spread in the flow domain. The induced electric currents interact with $\mathbf{B}$ giving rise to a non-uniform Lorentz force that brakes the fluid and creates vorticity.

Assuming that the only component of the applied field points in the z-direction, the dimensionless equations of motion take the form

$$\frac{\partial u}{\partial x} + \frac{\partial v}{\partial y} = 0, \tag{1}$$

$$\frac{\partial u}{\partial t} + u\frac{\partial u}{\partial x} + v\frac{\partial u}{\partial y} = -\frac{\partial p}{\partial x} + \frac{1}{\mathrm{Re}}\nabla_\perp^2 u + \frac{\mathrm{Ha}^2}{\mathrm{Re}} j_y B_z^0, \tag{2}$$

$$\frac{\partial v}{\partial t} + u\frac{\partial v}{\partial x} + v\frac{\partial v}{\partial y} = -\frac{\partial p}{\partial y} + \frac{1}{\mathrm{Re}}\nabla_\perp^2 v - \frac{\mathrm{Ha}^2}{\mathrm{Re}} j_x B_z^0, \tag{3}$$

where the subscript $\perp$ denotes the projection of the ∇ operator on the xy plane. Here the velocity components u and v are normalized by U, the pressure p by ρU^2, the electric current density components, j_x and j_y, by $\sigma U B_{\max}$ and the applied field B_z^0 by $B_{\max}$, where $B_{\max}$ is the maximum strength of the applied magnetic field. Dimensionless coordinates x and y are normalized by L, while the time t is normalized by L/U. The dimensionless parameter $\mathrm{Ha} = B_{\max} L\sqrt{\sigma/\rho\nu}$ and $\mathrm{Re} = UL/\nu$ are the Hartmann and Reynolds numbers, respectively, where ρ and ν are the mass density and the kinematic viscosity of the fluid, respectively.

Maxwell equations in the quasi-static approximation can be combined to give the induction equation. In the two-dimensional case, this equation reduces to a single equation for the component b_z, namely,

$$0 = \nabla_\perp^2 b_z - u\frac{\partial B_z^0}{\partial x} - v\frac{\partial B_z^0}{\partial y}, \tag{4}$$

where the induced magnetic field b_z has been normalized by $\mathrm{Rm}B_{\max}$. Once $\mathbf{b}$ is defined, the Ampere's law $\nabla \times \mathbf{b} = \mathbf{j}$ gives an expression to calculate electric currents. This equation also guarantees that the electric current density is divergence-free, $\nabla \cdot \mathbf{j} = 0$. Hence, the current density components are given by

$$j_x = \frac{\partial b_z}{\partial y}, \qquad j_y = -\frac{\partial b_z}{\partial z}. \tag{5}$$

Equations (5) show that the induced magnetic field serves as a stream function for the electric current in the plane of flow.

We use an analytic expression for the field produced by a magnetized square surface uniformly polarized at the normal direction [10]. In dimensional terms, placing the coordinate system in the centre of a rectangular surface with side lengths $X_0 = 2a$ and $Y_0 = 2b$, the normal component of the field produced by a single magnetized surface laying on the plane $Z = Z_0$, is given by

$$\begin{aligned}
\mathcal{B}_z^0 \;=\; & \alpha B_{\max}\left\{\tan^{-1}\left(\frac{(X+a)(Y+b)}{(Z-Z_0)[(X+a)^2+(Y+b)^2+(Z-Z_0)^2]^{1/2}}\right)\right. \\
& + \tan^{-1}\left(\frac{(X-a)(Y-b)}{(Z-Z_0)[(X-a)^2+(Y-b)^2+(Z-Z_0)^2]^{1/2}}\right) \\
& - \tan^{-1}\left(\frac{(X+a)(Y-b)}{(Z-Z_0)[(X+a)^2+(Y-b)^2+(Z-Z_0)^2]^{1/2}}\right) \\
& \left. - \tan^{-1}\left(\frac{(X-a)(Y+b)}{(Z-Z_0)[(X-a)^2+(Y+b)^2+(Z-Z_0)^2]^{1/2}}\right)\right\},
\end{aligned} \tag{6}$$

where $\mathcal{B}_z^0$ stands for the dimensional applied magnetic field and α is a normalization constant. We consider that the magnetized surface has a square shape, that is, $2a = 2b = L$. Therefore, L is taken as the geometrical length scale used to non-dimentionalize the flow variables. Further, we consider that the magnetized surface is located at $Z = -L$, that is, underneath the plane of flow. With this assumption, border effects due to the square shape of the magnetized plate are smoothed out in the plane of flow. Since in the 2D approximation the flow is restricted only to this plane, the dependence on the z-coordinate is disregarded. Equation (6) gives a symmetric distribution of the magnetic field with a maximum value at the centre of the plate and with a rapid decay as the distance from the centre increases.

We assume that far away from the applied magnetic field, a steady uniform flow in the positive x-direction is imposed. With the origin of coordinates located at the point of maximum magnetic field strength, the boundary conditions on the velocity components are

$$u \to 1, \quad v \to 0, \quad \text{as } x, y \to \pm\infty. \tag{7}$$

It is obviously expected that the strength of the induced magnetic field is higher near the zone, where the applied field is strong. As the distance from the source of the applied field grows, the induced field must decrease and vanish at infinity. Therefore, it must satisfy

$$b_z \to 0, \quad \text{as } x, y \to \pm\infty. \tag{8}$$

Further, both the velocity components and the induced magnetic field must in principle remain finite at the origin.

2. Creeping flow solutions. We first look for solutions, where the vorticity transport is dominated by diffusion. Under these conditions, a balance is established among pressure, Lorentz and viscous forces and the flow displays only steady laminar solutions.

2.1. Perturbation solution. With the aim to obtain analytic solutions, we first apply a perturbation approach. We simplify the equations of motion by assuming that the flow is only slightly perturbed by the Lorentz force. Therefore, the dimensionless velocity components can be expressed as

$$u = 1 + u', \quad v = v', \tag{9}$$

where u' and v' are the perturbations to the oncoming uniform flow due to the presence of the magnetic obstacle. This approximation will be valid provided that the Reynolds number is very small, namely, under creeping flow conditions. Assuming that $u', v' \ll 1$, in such a way their products with the $O(1)$ applied field derivatives can be neglected in (4), the magnetic induction equation reduces to

$$\nabla_\perp^2 b_z = \frac{\partial B_z^0}{\partial x}. \tag{10}$$

This equation is uncoupled from the velocity perturbations, therefore, at this approximation the induced field b_z is created by the unperturbed uniform flow. To find an analytic solution of equation (10) with the applied field given by (6) is a complicated task. For the sake of simplicity, the applied magnetic field is approximated through a Gaussian distribution,

$$B_z^0(x, y) = \sqrt{\frac{n}{\pi}}\, \mathrm{e}^{-n(x^2+y^2)}, \quad n > 0, \tag{11}$$

whose integral in the infinite domain is equal to 1. This magnetic field distribution approximates the field produced by a magnetic point dipole. Using (11), an analytical solution of Eq. (10) can be found that satisfies condition (8), namely,

$$b_z(x, y) = -\frac{1}{2\sqrt{n\pi}} \frac{x}{x^2 + y^2}\, \mathrm{e}^{-n(x^2+y^2)}. \tag{12}$$

However, as a consequence of the approximation, this solution diverges at the origin. Nevertheless, it closely reproduces the behaviour of the induced field, as can be shown from the numerical solution of the full equations. Fig. 1*a* shows the

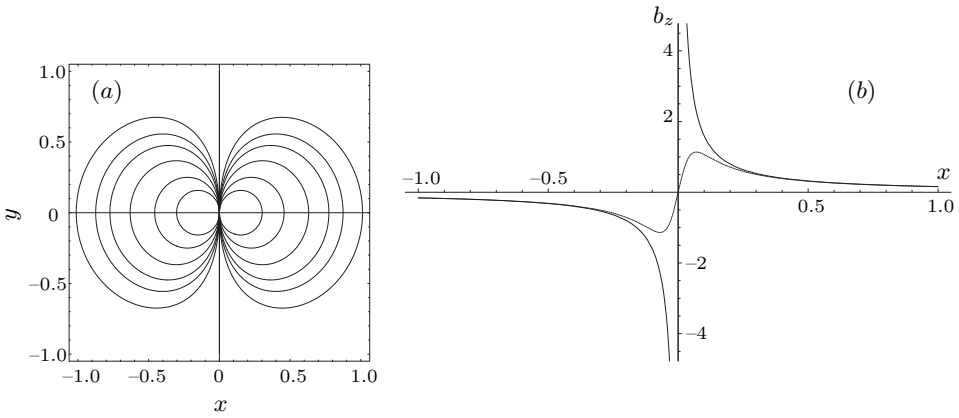

Fig. 1. (*a*) Isolines of the induced magnetic field in the creeping flow past a magnetic obstacle. (*b*) The induced field as a function of the axial coordinate at $y = 0$ (solid line) and $y = 0.1$ (dashed line). $n = 100$.

isolines of the induced magnetic field given by Eq. (12), while Fig. 1*b* presents the variation of b_z with respect to the streamwise coordinate. This reveals that the flow past the magnetic obstacle generates two symmetric current loops, upstream and downstream the location of the obstacle, with clockwise and anti-clockwise circulation, respectively. Hence, in the neighborhood of the origin, the flow of current in the negative direction is intensified. Due to the direction of the applied field, this results in a localized Lorentz force that opposes the fluid motion and causes an abrupt change in the pressure in the obstacle neighborhood.

The flow perturbation can be found through the solution of Eqs. (1)-(3). By introducing Eqs. (9) into (1)-(3) and neglecting second order products in the perturbed velocities, a linearized system of equations is obtained. Taking the curl, we get a transport equation for the only vorticity component, $\omega_z = \partial v'/\partial x - \partial u'/\partial y$. For a steady state with Re $<<$ 1, the vorticity can be expanded as $\omega_z = \omega_z^{(0)} +$ Re $\omega_z^{(1)} + O(\mathrm{Re}^2)$. Therefore, at $O(\mathrm{Re}^0)$ the vorticity satisfies

$$\nabla_\perp^2 \omega_z^{(0)} = \mathrm{Ha}^2 \left(j_x \frac{\partial B_z^0}{\partial x} + j_y \frac{\partial B_z^0}{\partial y} \right), \tag{13}$$

where conservation of current has been used. The right-hand side of Eq. (13) is known at the leading order of approximation since the current density components can be calculated explicitly from equations (5) and (12). The solution of Eq. (13) is found to be

$$\omega_z^{(0)}(x,y) = \frac{\mathrm{Ha}^2\, y}{4\pi(x^2+y^2)} \left[\frac{1}{2} \mathrm{e}^{-2n(x^2+y^2)} + n(x^2+y^2) Ei(-2n(x^2+y^2)) \right], \tag{14}$$

where

$$Ei(z) = -\int_{-z}^{\infty} \frac{\mathrm{e}^{-t}}{t} \mathrm{d}t, \quad \text{for } z > 0.$$

Solution (14) satisfies the condition $\omega_z \to 0$ as $x, y \to \pm\infty$ but, as the induced field (12), diverges at the origin. The assumption $u', v' \ll 1$ limits the solution to small values of the Hartmann number since the flow field cannot be substantially altered. In Figs. 2*a*,*b* the solution (14) is presented for Ha = 1. Fig. 2*a* shows the vorticity isolines, while Fig. 2*b* presents the vorticity as a function of the streamwise coordinate at different cross-stream positions. It is shown that symmetric regions of positive and negative vorticity are created due to the presence of the magnetic obstacle.

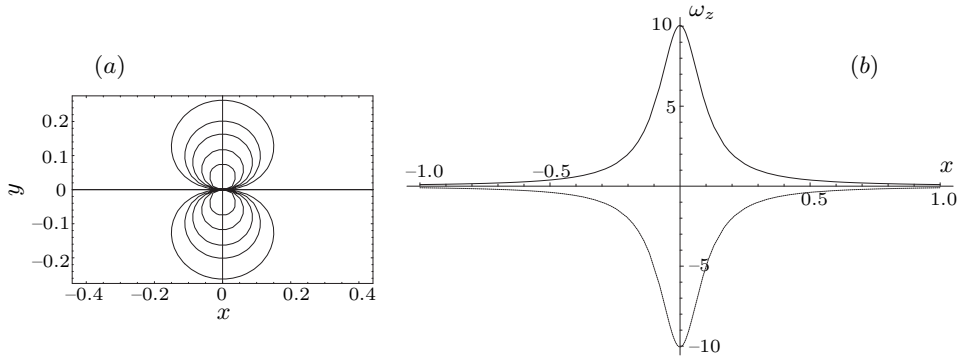

Fig. 2. (a) Vorticity isolines at $O(1)$ in the creeping flow past a magnetic obstacle. (b) Vorticity as a function of the axial coordinate at $y = \pm 0.1$. Ha = 1, $n = 100$.

2.2. Numerical solution. We implemented a numerical method in order to solve full equations (1)–(4) with the applied magnetic field (6). The numerical solution was addressed using a formulation based on the primitive variables, the velocity and pressure, and the induced magnetic field as an electromagnetic variable. A finite difference method on an orthogonal equidistant grid was used to solve the governing equations in a rectangular geometry, assuming a prescribed unform flow at the inlet and Neumann boundary conditions at the outlet. Symmetry-type conditions simulating a frictionless wall were imposed at the lateral boundaries, while the induced magnetic field was set to zero at the boundaries of the integration region. The details of the numerical method and its validation are given in [9]. First, we explored numerically the behaviour of the flow in the range $1 \leq \mathrm{Ha} \leq 100$ under the creeping flow conditions (Re = 0.05). In the range $1 \leq \mathrm{Ha} \leq 7$ the flow behaves mostly as the analytic solution predicts, namely, only two current loops exist and due to the Lorentz force, opposing the main flow, the pressure rises upstream as the obstacle is approached and drops suddenly downstream in a distance of the order of the characteristic length. This force causes a deficit in the streamwise velocity and the appearance of a small cross-stream component, which gives rise to a local shear flow that is more pronounced the higher the Hartmann number. As Ha grows, inner current loops appear inside the obstacle modifying the flow dynamics in a noticeable way (see Fig. 3a, where the projection of the magnetized surface on the plane of motion is shown through a unitary square for visualization purposes). Due to the stronger Lorentz force opposing the flow in the upstream fringing region the fluid circulates around the obstacle, increasing the cross-stream velocity components to reach the same order of magnitude as the streamwise com-

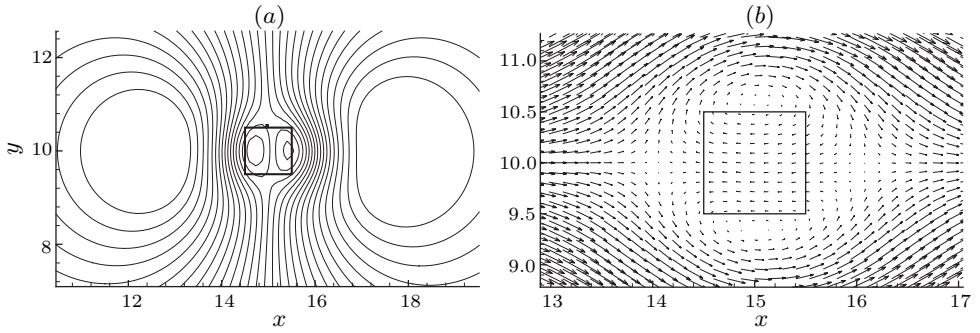

Fig. 3. (a) Induced magnetic field isolines. (b) Velocity field. Re = 0.05, Ha = 30.

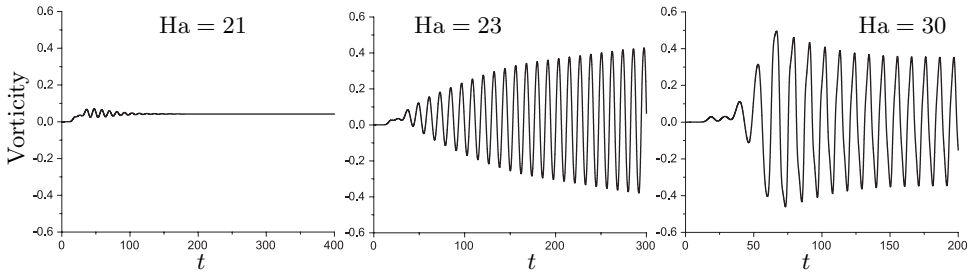

Fig. 4. Vorticity as a function of time in the centerline downstream the magnetic obstacle for different Hartmann numbers. Re = 100.

ponents and intensifying the shear layers formed in the lateral fringing regions. As a consequence, two tenuous recirculation zones (counter-rotating vortices) are formed (see Fig. 3*b*).

3. Convection dominated regime. We present here the numerical results for conditions, where convection is dominant, namely, Re = 100. We explored the range $1 \leq \mathrm{Ha} \leq 100$ and, under these conditions, the laminar flow may display either steady or time-dependent solutions. Three different laminar flow regimes were detected according to the value of the Hartmann number: steady, transition and periodic vortex shedding [9]. For Re = 100, a transition flow occurs in the range $20 \leq \mathrm{Ha} \leq 25$, where the flow develops a time periodic behaviour characterized by the formation of elongated vortices in the near wake that are eventually shed. The periodic flow has been characterized by analyzing the time dependence of vorticity in the wake. Fig. 4 shows the vorticity as a function of time in the axial midline at a position of 15 units downstream the centre of the obstacle, for different Hartmann numbers. For Ha = 21, an incipient oscillation that eventually is damped out is deteced along with a very weak recirculation in the near wake. As Ha increases, the oscillation is sustained with a growing amplitude; the periodic vortex shedding is fully established for Ha > 25. Fig. 5 shows instantaneous vorticity isocontours for Ha = 30. Initially, the formation of shear layers at both sides of the obstacle is promoted. They remain parallel and aligned with the main flow direction, displaying maximum and minimum of vorticity a few units

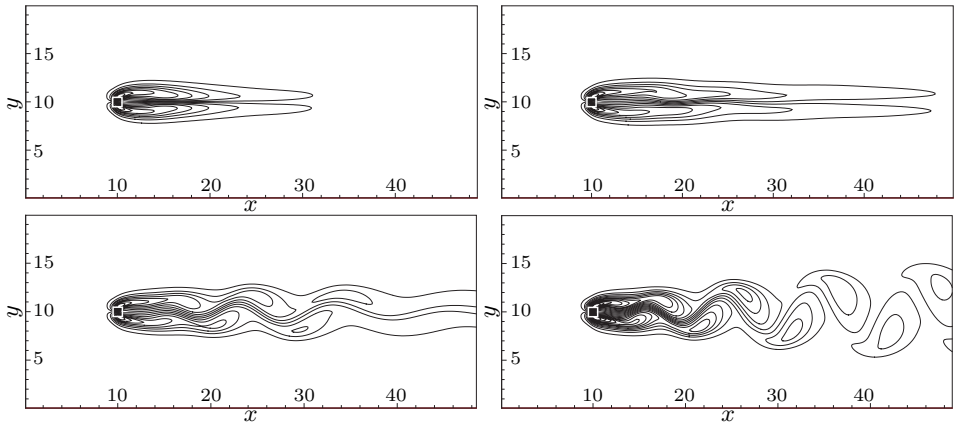

Fig. 5. Instantaneous isolines of vorticity at times t = 25, 50, 75 and 100, respectively. Re = 100, Ha = 30.

downstream the obstacle center. As the flow travels downstream, the shear layers become unstable. The onset of the instability is featured by the appearance of a transverse oscillation in the mid horizontal axis along the wake. The instability first appears far downstream from the magnetic obstacle, where both the applied and the induced magnetic fields are negligible. This means that the instability is related to the specific shape of the velocity profile, which is formed by the action of the magnetic field near the obstacle. A periodic wake similar to the von Kármán vortex street formed behind a cylinder is observed. The Strouhal number that characterizes the vortex shedding was close to 0.1, which differes from values around 0.150 usually reported for the two-dimensional flow past a cylinder for this Reynolds number. The Strouhal number exhibits a weak dependence on Ha, similarly to the behaviour observed in other MHD flows, where the vortex shedding phenomenon appears [2, 4].

4. Conclusions. The main objective of this work is to draw attention to the generation of vorticity and the eventual appearance of instabilities leading to unsteady generation of vortices in flows under non-uniform magnetic field distributions. This has immediate implications for heat transfer enhancement applications. The key aspect of the flow analysis is the consideration of inertial effects and the existence of electromagnetic non-uniformities given by the applied magnetic field gradients. The numerical results have shown that this problem has many similarities with the flow around bluff bodies, displaying steady as well as time-periodic vortical flow regimes.

Acknowledgements. Financial support from UC MEXUS-CONACYT Faculty Fellowship Program and Project IN111705 UNAM is gratefully acknowledged.

REFERENCES

[1] Y. Kolesnikov, A. Tsinober. Two-dimensional turbulent flow behind a circular cylinder. *Magnetohydrodynamics*, vol. 8 (1972), no. 3, pp. 300–307.

[2] B. Mück, C. Günther, U. Müller, L. Bühler. Three-dimensional MHD flows in rectangular ducts with internal obstacles. *J. Fluid Mech.*, vol. 418 (2000), pp. 265–295.

[3] A. Alpher, H. Hurwitz, R.H. Johnson, D.R. White. Some studies of free-surface mercury magnetohydrodynamics. *Rev. Mod. Phys.*, vol. 32 (1960), pp. 758–769.

[4] L. Bühler. Instabilities in quasi-two-dimensional magnetohydrodynamic flows. *J. Fluid Mech.*, vol. 326 (1996), pp. 125–150.

[5] U. Müller, L. Bühler. *Magnetofluiddynamics in channels and containers* (Springer, Berlin, 2001).

[6] H. Honji. Wavy wake formation in the absence of submerged bodies in electrolyzed salt water. *J. Phys. Soc. Japan*, vol. 60 (1991), no. 4, pp. 1161–1164.

[7] H. Honji, Y. Haraguchi. Electrolytically induced quasi-two-dimensional vortex pairs. *J. Phys. Soc. Japan*, vol. 64 (1995), no. 7, pp. 2274–2277.

[8] Y.D. Afanasyev, V.N. Korabel. Wakes and vortex streets generated by translating force and force doublet: laboratory experiments. *J. Fluid Mech.* vol. 553 (2006), pp. 119–141.

[9] S. Cuevas, S. Smolentsev, M. Abdou. On the flow past a magnetic obstacle. *J. Fluid Mech.* vol. 553 (2006), pp. 227–252.

[10] M. McCaig. *Permanent magnets in theory and practice* (Wiley, New York, 1977).

Received 27.04.2006